NeuroImage: Clinical 24 (2019) 101956

Contents lists available at ScienceDirect

NeuroImage: Clinical

journal homepage: www.elsevier.com/locate/ynicl

Neural activation and connectivity during cued eye blinks in Chronic Tic Disorders

Sandra K. Loo[a,*], Makoto Miyakoshi[b], Kelly Tung[a], Evan Lloyd[a], Giulia Salgari[a], Andrea Dillon[a], Susanna Chang[a], John Piacentini[a], Scott Makeig[b]

[a] Semel Institute for Neuroscience and Human Behavior, University of California, Los Angeles, 760 Westwood Plaza, Los Angeles, CA 90095, United States of America
[b] Swartz Center for Neural Computation, University of California, San Diego, 9500 Gilman Drive, La Jolla, CA 92093-0559, United States of America

ARTICLE INFO

Keywords:
Tourette syndrome
EEG
Pediatric
Gamma power
Attention network

ABSTRACT

Objective: The pathophysiology of Chronic Tic Disorders (CTDs), including Tourette Syndrome, remains poorly understood. The goal of this study was to compare neural activity and connectivity during a voluntary movement (VM) paradigm that involved cued eye blinks among children with and without CTDs. Using the precise temporal resolution of electroencephalography (EEG), we used the timing and location of cortical source resolved spectral power activation and connectivity to map component processes such as visual attention, cue detection, blink regulation and response monitoring. We hypothesized that neural activation and connectivity during the cued eye blink paradigm would be significantly different in regions typically associated with effortful control of eye blinks, such as frontal, premotor, parietal, and occipital cortices between children with and without CTD.

Method: Participants were 40 children (23 with CTD, 17 age-matched Healthy Control [HC]), between the ages of 8–12 (mean age = 9.5) years old. All participants underwent phenotypic assessment including diagnostic interviews, behavior rating scales and 128-channel EEG recording. Upon presentation of a cue every 3 s, children were instructed to make an exaggerated blink.

Results: Behaviorally, the groups did not differ in blink number, latency, or ERP amplitude. Within source resolved clusters located in left dorsolateral prefrontal cortex, posterior cingulate, and supplemental motor area, children with CTD exhibited higher gamma band spectral power relative to controls. In addition, significant diagnostic group differences in theta, alpha, and beta band power in inferior parietal cortex emerged. Spectral power differences were significantly associated with clinical characteristics such as tic severity and premonitory urge strength. After calculating dipole density for 76 anatomical regions, the CTD and HC groups had 70% overlap of top regions with the highest dipole density, suggesting that similar cortical networks were used across groups to carry out the VM. The CTD group exhibited significant information flow increase and dysregulation relative to the HC group, particularly from occipital to frontal regions.

Conclusion: Children with CTD exhibit abnormally high levels of neural activation and dysregulated connectivity among networks used for regulation and effortful control of voluntary eye blinks.

1. Introduction

Chronic Tic Disorders (CTDs), including Tourette's Disorder, affect approximately 20–30% of children, with worldwide prevalence of CTDs estimated at 1–2% (Schlander et al., 2011). Although the natural history of CTDs is not well studied, tics continue into adulthood for up to 50% of individuals (Bloch et al., 2006). CTDs are associated with increased rates of comorbid psychopathology, most often ADHD and OCD (Specht et al., 2011), as well as considerable distress, elevated levels of suicidal ideation, discrimination, and social and academic impairment across the lifespan (Scahill et al., 2005; Storch et al., 2015).

Despite a building research base on this neurodevelopmental disorder, numerous recent reviews agree that the etiology and pathophysiology of CTDs remain poorly understood (Hashemiyoon et al., 2017). Thus far, convergent data from genetics, neuroimaging, neurochemical, and neuropsychological studies have implicated cortico-striatal-thalamo-cortical circuits as underlying tic generation in CTDs (Ganos et al., 2013). In addition to the cortico-thalamic network, interactions between and among several other neural circuits have been implicated. For example, the fronto-parietal attention, cingulo-opercular, and

* Corresponding author.
E-mail address: Sloo@mednet.ucla.edu (S.K. Loo).

https://doi.org/10.1016/j.nicl.2019.101956
Received 7 July 2018; Received in revised form 6 May 2019; Accepted 20 July 2019
Available online 27 July 2019

somatosensory networks have been implicated in playing a role in the basic pathophysiology and pathogenesis of CTDs (Church et al., 2009). Published electroencephalography (EEG) and event-related potential (ERP) studies in CTDs have been largely consistent with neuroimaging findings and report deviations in cortical activity patterns in frontal and sensorimotor regions (Serrien et al., 2005; Thibault et al., 2009; Yordanova et al., 2006). Recent treatment studies of deep brain stimulation for CTD suggest that thalamic gamma band synchronization and theta-gamma cross frequency coupling may be important biomarkers of tic severity (Maling et al., 2012). Collectively, data suggest that aberrant activity in more than one neural circuit occurs in CTDs, however, findings are confounded by small (usable) sample sizes, developmental differences across wide subject age ranges, potential medication effects, and the uncontrolled presence of psychiatric comorbidities.

One method for studying the interaction of brain networks involved in attention, task control and movement has been to use voluntary movements, such as finger tapping and blink suppression paradigms. Voluntary movement is an interesting paradigm to study CTDs for several reasons. First, although CTDs primarily involve involuntary movement, there is a voluntary aspect in that most individuals with CTD are able to voluntarily suppress their tics for varying lengths of time and that tic expression is sensitive to environmental factors (Piacentini and Chang, 2006). This suggests some level of conscious control over movement is in play in CTDs. Second, studies suggest that there is continuity in neural circuitry underlying voluntary movement and urge suppression among individuals with and without CTD. For example, it is hypothesized that the inhibitory control exerted by frontal structures such as dorsolateral prefrontal cortex (DLPFC), inferior frontal gyrus (IFG), and supplemental motor area (SMA) during voluntary movement and self-regulation is consistent with neural activity reported during tic inhibition and suppression (Deckersbach et al., 2014; Ganos et al., 2014; Roessner et al., 2011). Finally, eye blinking in particular, is a naturally occurring phenomena that occurs in all people, but is one of the most frequently reported tics that often occurs with premonitory urge (McGuire et al., 2015); blink suppression paradigms have been successfully employed to examine neural correlates of urge in control populations (Berman et al., 2011).

Studies of healthy adults report that the neural correlates of voluntary eye blinking are activations in multiple areas of the frontal lobe, including the medial frontal gyrus, superior frontal gyrus, medial precentral gyrus and supplemental motor area (SMA), as well as the posterior parietal cortex (PPC), and occipital cortices (Berman et al., 2011; Bodis-Wollner et al., 1999; Chung et al., 2006). In addition, numerous studies have suggested that the SMA, in coordination with motor and parietal cortices, is critically involved in voluntary movement preparation, action planning, and intentional blinking (Chung et al., 2017; Franzkowiak et al., 2012). EEG studies of voluntary motor movements (primarily finger tapping or large muscle movements) report parietal alpha- and beta-band spectral power decrease (which is thought to be associated with activation of underlying cortex) and increased coherence and effective connectivity between parietal, SMA and motor areas across broad band frequency ranges (Chung et al., 2017; Franzkowiak et al., 2012; Franzkowiak et al., 2010). Overall, voluntary blinking is associated with a widely distributed cortical network of frontal, motor, parietal and occipital regions.

When healthy adults were asked to suppress, regulate or control eye blinks, a network of brain regions overlapping with voluntary blinking such as superior/medial frontal gyrus, precentral gyrus and SMA was activated, but also involved unique neural regions such as inferior frontal gyrus (IFG), dorsolateral prefrontal cortex (DLPFC), cingulate gyrus, precuneus, inferior parietal lobe, fusiform gyrus, and sensory association areas (Chung et al., 2006; Abi-Jaoude et al., 2018). Poor performance (escape blinks or poor suppression) was associated with activation of several areas including anterior cingulate cortex (ACC), paracentral lobule (SMA), inferior parietal lobule (IPL), angular gyrus, and precuneus (Abi-Jaoude et al., 2018). To our knowledge, there have not been any studies examining voluntary eye blinks or eye blink inhibition in typically developing children or individuals with Chronic Tic Disorders of any age.

While activation and connectivity within the visual system (i.e., fronto-occipital) pathway has not been extensively studied in CTDs, individuals with CTD have been noted to have smaller inferior occipital volumes relative to controls (Peterson et al., 2001) and decreased white matter volume in left lingual gyrus (Liu et al., 2013). In addition, aberrant visual area connectivity has been noted among individuals with CTDs. A recent study reported reduced nodal efficiencies in several occipital regions (inferior occipital gyrus and lingual gyrus) that are important for visual processing (Wen et al., 2017). DTI studies provided direct evidence for disrupted structural integrity in various WM tracts in children with CTD, including the superior and inferior fronto-occipital fasciculus (Wen et al., 2016), which are the bases for structural connectivity between the occipital and frontal regions. Weak fronto-occipital connectivity may be, at least in part the reason for weaknesses in the integration of visual inputs and organized motor outputs that have been noted among children with CTDs (Como, 2001). The time course of the fronto-occipital activation and connectivity is not well delineated given that most studies use MRI or are structural in nature. The current study will use the precise timing of electroencephalography (EEG) to allow parsing of the time course of neural activation and connectivity between frontal, motor, parietal and occipital pathways during the cognitive processing stages leading up to the blink response.

The goal of the current study was to investigate the neural processes underlying a cued (as opposed to self-paced) voluntary movement that replicate a common tic behavior - an exaggerated eye blink - among children with and without CTDs. To address the challenge of movement limitations inherent in traditional brain imaging methods, we used a new approach, mobile brain/body imaging (MoBI) (Delorme et al., 2011), which allows movement of the head and body to occur during simultaneous EEG recording (Gwin et al., 2011), to characterize neural circuitry involved in CTDs. Both temporally resolved oscillatory activity as well as functional connectivity at the cortical source level were examined with the hypothesis that children with CTD would exhibit significantly higher activation and increased connectivity between regions that are associated with blink regulation and control among healthy adults such as the DLPFC, SMA, sensorimotor cortex, inferior parietal lobule, and occipital cortex. We will further use the precise time resolution of EEG to disentangle subcomponent processes involved in the cued blink task, starting with visual processing of the cue through blink initiation and response monitoring along classic neural pathways associated with effortful voluntary movements (Roessner et al., 2013).

2. Method

2.1. Sample

Participants were 40 children (23 with CTD, 17 Healthy Control [HC]), between the ages of 8–12 years old. Children were recruited from the community through radio and newspaper advertisements. After receiving verbal and written explanations of study requirements, and prior to any study procedures, all parents/participants provided written informed consent/assent as approved by the Institutional Review Board.

2.2. Procedures

All participants underwent diagnostic interviews and EEG recording. Psychiatric diagnoses were determined using a semi-structured diagnostic interview, the Anxiety Disorder Interview Schedule, Child Version (ADIS) (Silverman and Albano, 1996), modified to cover Tourette and other tic disorders (Walkup et al., 2008), and administered by trained and carefully supervised graduate level psychologists.

The ADIS was supplemented by the clinician-administered Yale Global Tic Severity Schedule (YGTSS) (Leckman et al., 1989), Child Yale-Brown Obsessive-Compulsive Scale (CYBOCS) (Scahill et al., 1997), and Premonitory Urge for Tics Scale (PUTS) (Woods et al., 2005). To assess and quantify broad-band behavioral functioning, parents completed the Child Behavior Checklist (CBCL) (Achenbach, 2000) and the Behavior Rating of Individual Executive Functions (BRIEF) (Gioia et al., 2002). Senior clinicians (JP, SC) confirmed the presence of DSM-5 psychiatric diagnoses after individual review of each participant's symptoms, duration, and impairment level. Estimated intelligence (IQ) was assessed using the Wechsler Abbreviated Scale of Intelligence (WASI) (Weschler, 1999).

Subjects were excluded from participation if they were positive for any of the following: head injury resulting in concussion, diagnoses of autism, major depression, bipolar disorder, panic disorder or psychosis, estimated Full Scale IQ $<$ 80 or YGTSS $<$ 15 (CTD only). In addition, HC subjects were excluded if they had any major Axis I diagnosis or were on any type of psychoactive medication. CTD subjects with comorbid ADHD on stimulant medication discontinued use for 24 h prior to their visit.

2.3. Experimental task

All children were instructed to perform a 3.5-min cued voluntary movement (VM) task, during which they were instructed to make an exaggerated blink each time they saw the visual cue, which was a yellow dot 2-cm in diameter, shown on a 21.5-in screen with 1280 × 1024 resolution, and presented 70 times, every 3-s (stimulus duration = 1000-ms, ISI = 2000 ms). All children were observed to successfully practice and subsequently perform the VM on cue. Furthermore, the number of blinks exhibited during the task was tested at the group level to ensure equivalent performance across groups. This VM was chosen over others (i.e., finger tapping) because it approximates a common motor tic, therefore increasing the relevance to CTDs.

2.4. EEG recording

EEG signals were recorded using the Electrical Geodesics Incorporated (EGI) hardware and software with 128 Hydrocel electrodes in an extended International 10/10 configuration. Data were sampled at 1000 samples per second, referenced to Cz and impedance threshold was set at 50 kΩ (per manufacturer standard). Eye movements were monitored by electrodes placed above the eyes for vertical eye movements and on the outer canthus of each eye for horizontal movements (REOG, LEOG). Facial electromyography (EMG) leads were placed on the cheeks bilaterally over the zygomaticus major muscles. Key head landmarks (nasion, preauricular notches) and 3-D electrode locations were recorded via Polhemus, Inc. Raw EEG with embedded event markers (VM cue) was recorded using the Lab Streaming Layer (https://github.com/sccn/labstreaminglayer), which allows integration of multiple information streams, which is critical to the MoBI approach (Delorme et al., 2011).

2.5. EEG analysis

2.5.1. Overview

Data processing relied primarily on two complementary techniques for artifact correction: artifact subspace reconstruction (ASR) (Mullen et al., 2015) and independent component analysis (ICA) (Makeig et al., 1996). ASR removes and interpolates linear components of non-stationary artifacts using a sliding window and principal component analysis (PCA), while the subsequent ICA captures stationary brain and non-brain (i.e., artefactual) source activities. To characterize changes in EEG power across time (i.e., time-frequency power analysis), event-related spectral perturbation (ERSP) was computed using Morlet wavelet transform to indicate time-frequency characteristics of the decomposed event-related potential. In parallel, to characterize effective connectivity among independent component source activations, renormalized partial directed coherence (rPDC) (Schelter et al., 2009) was computed.

2.5.2. Preprocessing

The EEG data analyses were carried out in EEGLAB (Delorme and Makeig, 2004) with plugin tools. Separate preprocessing pipelines were applied for ERSP and connectivity analyses (see Supplemental Materials S1). In short, data were down sampled to different sampling rates (250 Hz vs. 100 Hz) with different anti-aliasing filter parameters for ERSP and connectivity analyses, respectively (Barnett and Seth, 2011).

2.5.3. Artifact subspace reconstruction (ASR)

EEGLAB plugin *clean_rawdata()* was used to de-noise continuous channel data (Mullen et al., 2015). The process includes: 1) Removing channels with flat signal longer than 5 s; 2) Removing channels that were poorly correlated (r $<$ 0.85) with adjacent channels; 3) Applying ASR to remove and interpolate non-stationary high-amplitude bursts (see Supplemental Materials S2 for details). This process improved data stationarity, which is an assumption for the subsequent ICA.

2.5.4. Independent component analysis

Adaptive mixture independent component analysis (AMICA) (Palmer et al., 2006, 2007) was applied (see Supplemental Materials S3 for parameters). Equivalent current dipoles were estimated using Fieldtrip (Oostenveld et al., 2011) for scalp projections of the independent components (ICs). Brain ICs were selected if the estimated dipolar source was inside the brain and had $<$ 15% residual variance (see Supplemental Materials S4 for details).

2.5.5. Time-frequency analysis – group-level ERSP

The continuous IC activations were epoched from −4 to 4 s relative to visual cue onset to blink. Out of 60 trials, 54–56 trials were left for HC and CTD groups on average for final analysis. Using the EEGLAB STUDY framework, k-means algorithm was applied on dipole location (dimension, 3; weight, 10) and frequency spectrum (3–50 Hz). EEGLAB's default blend of Morlet wavelet transform and short-term Fourier transform was performed using a 3.34-s sliding window to generate time-frequency data from −2.3 to 2.3 s (11.6 ms step) relative to stimulus onset and from 1 to 60 Hz (log-scaled 50 bins) while linearly increasing the number of cycles from 3 to 15 as the bin frequency increased. The single-trial values were averaged and converted to decibel (dB) unit; baseline was mean power between −1 and 0 s.

2.6. Connectivity analysis

We computed the multivariate autoregressive (MVAR) model across ICA-derived effective EEG sources using Source Information Flow Toolbox (SIFT) (Delorme et al., 2011). Although we hypothesized increased connectivity within the neural network involved in effortful control of eye blinks, these results were derived on healthy adults and it was unclear whether they were generalizable to children with and without CTD; thus whole brain connectivity was calculated. The data were epoched to −1 to 2 s relative to stimulus onset. The length of the sliding window length was 1-s, window step size was 20 ms, and there were 30 log-scaled frequency bins from 2 to 45 Hz. Vieira-Morf algorithm was used to fit a parametric MVAR model. This generated 100 data points from −0.5 to 1.5 s relative to stimulus onset. To compute causal connectivity, rPDC (Schelter et al., 2009) was computed to estimate multivariate information flow (see Supplemental Materials S6 for details).

The locations of ICs were smoothed with a 3-D Gaussian kernel with full-width at half maximum (FWHM) at 20 mm, which transformed the dipole locations into probabilistic dipole density. The dipole density was then segmented into 76 anatomical cortical regions of interest

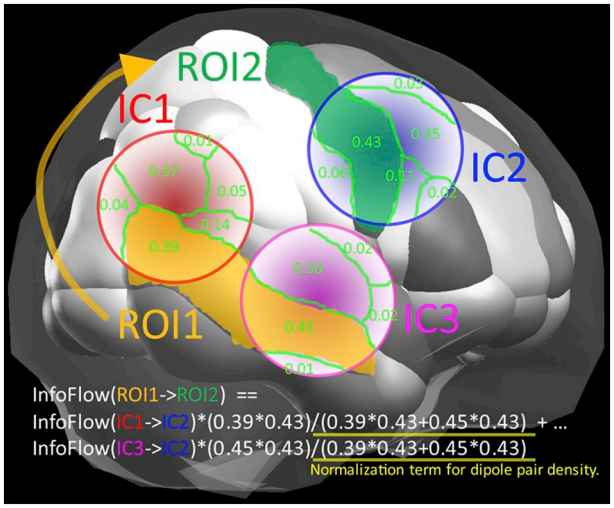

Fig. 1. Computation of source-level connectivity. This schematic illustrates the anatomical normalization of dipole-represented independent components (ICs) and computation of pairwise dipole density across anatomical regions of interest (ROIs).

(ROI) defined by the automated anatomical labeling atlas (AAL) (Tzourio-Mazoyer et al., 2002), which originally supported 88 regions that were slightly modified for use in EEG by re-organizing 12 sub-cortical regions, including limbic and basal structures, into 'upper basal' and 'lower basal' for right and left hemispheres. This was to done to retain sub-cortical, deep dipoles in the analyses, even though they are extremely difficult to measure with EEG and are not well modeled by ICA. Then, we computed anatomical ROI-to-ROI pairwise dipole density weighted with rPDC, which generated a connectivity matrix consisting of 76 × 76 graph edges. Self-connections were excluded. Thus, each participant was associated with a four-dimensional tensor of 76 [ROIs, origins] x 76 [ROIs, destinations] x 30 [frequency bins] x 100 [time points]. The tensors from individual participants were concatenated for each group, upon which graph edges were pre-selected so that a minimum 80% of unique participants had non-zero dipole density in a ROI after truncating the Gaussian distribution to 3 sigma, yielding a radius of 25.5 mm. The group comparison was performed on the overlapping graph edges between the groups (see Fig. 1).

2.7. Statistical tests

For both the ERSP and the weighted rPDC, a two-sample *t*-test was used to generate the initial t-score maps masked with an uncorrected $p < .01$. For multiple comparison correction, family-wise error rate (FWER) control, also known as cluster-level correction (Groppe et al., 2011a; Groppe et al., 2011b), was performed using permutation test with $p < .05$ threshold (see Supplemental Materials S7). Note that the surrogate data, which in the current context of FWER is called 'mass of cluster', were pooled across all edges so that 2.5th percentile and 97.5th percentile values of the total distribution were applied to correct *all* the edges and provide control of overall familywise error in any time-frequency plot of cluster/graph edge. MANCOVA and partial correlation analyses controlling for covariates such as age and psychiatric co-morbidity were run in SPSS v.23. Finally, movies were generated to visually explore group differinces in the temporal dynamics and spatial structure of event-related effective connectivity.

3. Results

3.1. Sample demographics and clinical characteristics

As seen in Table 1, the two groups did not differ in age or IQ. There was a trend towards a gender disparity between the two groups, with the HC group having a lower percentage of males relative to the CTD. The EEG data were subsequently tested for gender differences, no significant effects emerged for any measure (all *p*'s > .20); nonetheless, gender was included as a covariate in the analytic models.

Table 1
Sample demographics and clinical characteristics.

	HC	CTD
	M (SD)	M (SD)
N	17	23
Age, years	9.8 (1.7)	9.7 (1.6)
Sex, % males^	42%	73%
Estimated IQ	114 (15)	116 (113)
CBCL total*	42.1 (9.7)	53.7 (12.5)
CYBOC total*	0	10.9 (9.6)
YGTSS total*	0	25 (8.5)
PUTS urge presence*	0	4.4 (2.2)
PUTS urge strength*	0	4.1 (2.0)
PUTS tic frequency*	0	4.5 (2.3)
Co-morbid OCD*	0	39%
Co-morbid ADHD*	0	31%
Tourette disorder*	0	74%
Chronic motor tic disorder*	0	21%
Chronic vocal tic disorder*	0	5%
Taking psychotropic medications*	0	26%

HC = Healthy Control, CTD = Chronic Tic Disorder, IQ = intelligence, CBCL = Child Behavior Checklist, CYBOC = Child Yale-Brown Obsessive-Compulsive Scale; YGTSS = Yale Global Tic Severity Schedule; PUTS = Premonitory Urge for Tics Scale; OCD = Obsessive Compulsive Disorder, ADHD = Attention Deficit Hyperactivity Disorder.
* $p < .05$.
^ $p < .10$

3.2. Blink validation

Behavioral characteristics of the cued blink task for CTD and HC groups are shown in Fig. 2. The mean number of blinks and blink latency were not significantly different in the CTD and HC groups (*p*'s > .35). The visual inspection of the histogram (Fig. 2a) showed that the peaks of the both groups are nearly overlapping. Thus, the CTD group did not exhibit significantly more extraneous blinks, despite 12 out of 23 CTD subjects having a reported eye-blink tic and CTD subjects were not explicitly instructed to suppress any tics, including blinks. This data suggests that eye blinks may have been entrained during the task resulting in suppression of extra blink tics.

Next, we tested group differences in blink ERP amplitude at the channel level for differences in the duration and intensity of the emitted blinks. For this purpose, the computed ICA weight matrices from the final results were transferred to the minimally processed raw data (for complete preprocessing steps, see Supplemental Materials S5). To confirm blink ERPs on peri-occular channels, we selected the frontal five channels on the forehead (Fig. 2b) and calculated the blink ERP with minimally-processed raw data. In addition, to demonstrate that this large-amplitude blink ERP is efficiently modeled by ICA (being modeled as independent component means it can be subtracted later without affecting other independent components that represent various brain activities), we calculated the blink ERP with the three far-frontal EOG-IC clusters that accounted for 93% of ERP variance across the groups. Finally, we plotted the fully-cleaned data that were used for the final statistical comparison. The results showed that the ERP waveforms of the raw data and the back projection of the identified EOG-IC clusters were almost completely overlapped for both groups, indicating that these high-amplitude blink ERPs were mostly due to the contributions by the EOG-IC clusters identified. The ERP plots in Fig. 2c, d show a time window of 0–3000 ms relative to blink cue onset (which is the same length as each cued blink trial) and the baseline window was

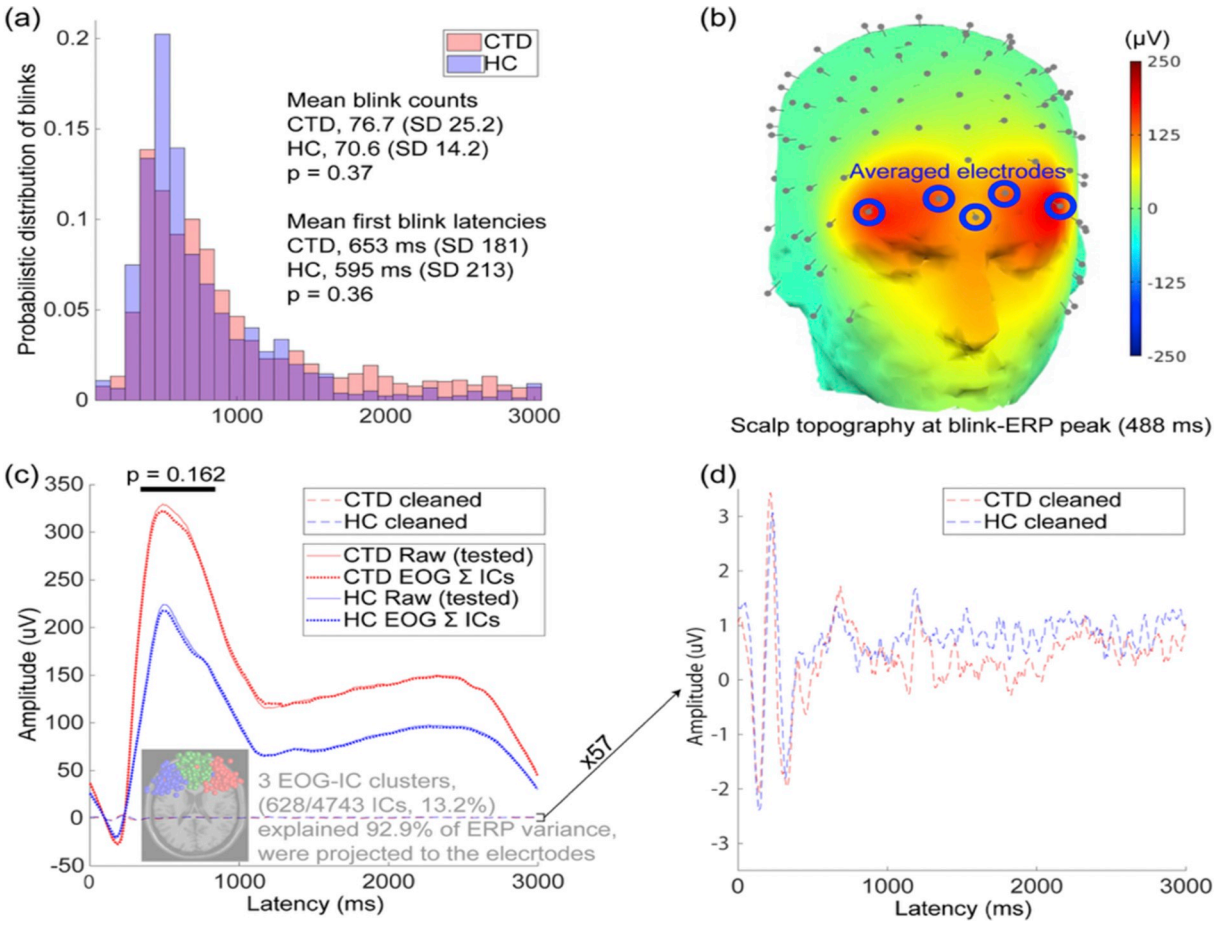

Fig. 2. Blink validation analyses indicate no significant group differences in blink number, latency, or ERP amplitude in raw and cleaned EOG data. (a) Histogram of blink latency shows probabilistic distribution of blink occurrence within a trial. Each bin is 100 ms and the sum of all binned values is 1 for each group. There were no significant group differences in blink count or latency. (b) A whole-head topography at the the blink ERP peak (group average = 488 ms) and locations of five frontal EEG electrodes used for analysis. (c) Blink ERP of minimally-processed raw data (see Supplemental Materials S5) show no significant group difference in ERP mean peak-window amplitude (indicated by dark line above the ERP peak). The dotted line (~0 uV) shows the back projected potentials at the same frontal electrodes from the three frontal EOG-IC clusters, which account for 13% of total ICs but 93% of the blink ERP. (d) Magnification (57 ×) of the cleaned EOG-IC data indicates overlap of the blink ERP for both groups. CTD = Chronic Tic Disorder, HC = Healthy Control, ERP = event related potential, EOG = Electroculography, IC = independent component.

0–100 ms (i.e., the mean value within this window was subtracted from all the data points). The blink ERP peak window was visually defined to be from 338 to 838 ms (group-average ERP peak latency = 488 ms), and mean ERP amplitudes within the window were not significantly different across groups (p = .16). These data indicate that both groups successfully performed the cued blink task with no significant diagnostic group differences in number, latency, or amplitude of blinks.

3.3. Brain oscillatory activity during cued voluntary movement

Having confirmed similar performance of the cued eye-blink, analyses of brain oscillatory activity resulted in a 15-cluster cortical source resolved solution (see Supplemental Materials S8 for scalp map and anatomical locations and S9 for channel-level ERP waveforms and scalp topographies). The CTD and HC groups differed significantly in spectral power within regions associated with blink control, such as DLPFC and SMA, and inferior parietal lobe (Abi-Jaoude et al., 2018). Clusters with centroid dipoles in bilateral motor cortices and visual cortices (mid and lateral occipital) were present in the 15-cluster solution, however, there were no significant group differences in spectral power between children with and without CTD. Thus, brain oscillatory activities in motor and visual clusters were not further examined.

Group differences in spectral power emerged primarily in the left DLPFC, SMA, inferior parietal and posterior cingulate sources (see Fig. 3). Differential activation began just after the VM cue with significant gamma power differences in SMA and posterior cingulate cortex (p < .05, corrected; Fig. 3a, c). Specifically, CTD individuals exhibited stronger gamma band (30–50 Hz) event-related increase (ERI) compared to the HC group, suggesting increased activation in response to the cue in the SMA and posterior cingulate cortex. Group differences in gamma power in the left DLPFC occurred largely after the blink occurred (Fig. 3b) suggesting differential response evaluation processes by diagnostic group. Alpha power decrease in the posterior cingulate at ~2000 ms post-cue for the CTD group (Fig. 3a) may indicate heightened visual-spatial attention, motor planning, and executive motor control as well as interoceptive processing compared to the HC group (Abi-Jaoude et al., 2018; Deiber et al., 2012; Leech and Sharp, 2014; Lerner et al., 2009). Finally, the HC group exhibited inferior parietal alpha band event-related decrease (ERD) (Fig. 3d) before, during and after the cued blink, whereas the CTD individuals had attenuated alpha ERD and alpha- and beta-band spectral power ERI during blink execution and response evaluation (500–1500 ms). These results remained significant when analyses were re-run using gender, ADHD and OCD comorbidity, and medication status as covariates.

In order to guide functional interpretation of the brain oscillatory activity differences between groups, Pearson correlations using all subjects were run between behavioral functioning measures and significant voxels of spectral power in the four cortical sources. In Table 2,

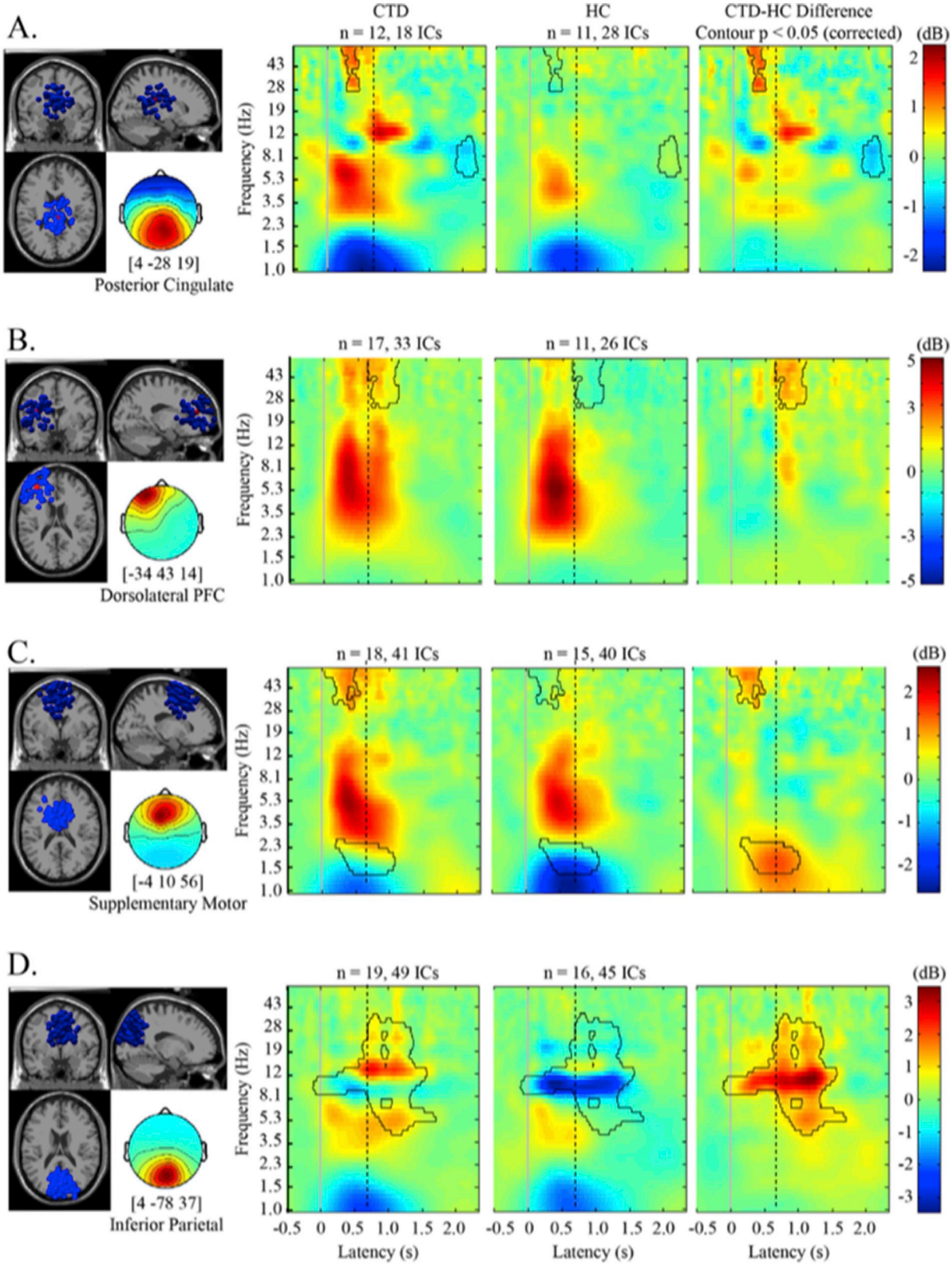

Fig. 3. Group differences in oscillatory activity during cued eye blink initiation and execution. Significant differences in spectral power were apparent in frontal, premotor, and parietal regions. Outlined in black are pixels significant at $p < .05$, corrected. Solid line at latency = 0 is blink cue onset. Dotted line indicates the group mean for blink latency. CTD = Chronic Tic Disorder, HC = Healthy Control, Post Cing = Posterior Cingulate, DLPFC = Dorsolateral prefrontal cortex, SMA = supplemental motor area, Inf = inferior, Hz = hertz, dB = decibel.

Table 2
Behavioral correlates of EEG activity during voluntary movement.
Frontal and parietal EEG activity that differed across groups were significantly associated with tic severity, premonitory urge, and emotion regulation.

Measure	Scale	DLPFC	SMA		Inf parietal	Left parietal		Right parietal		Posterior cingulate	
		Gamma	Gamma	Delta	Alpha	Beta	Alpha	Beta	Alpha	Gamma	Alpha
YGTSS	Total	**0.49***	**0.68****	0.28	**0.47****	**0.44***	**0.44***	0.24	0.20	**0.57****	**−0.54***
YGTSS	Impairment	**0.52****	**0.55****	0.22	**0.48****	0.38	**0.43***	0.33	0.23	**0.50***	**−0.61****
PUTS	Urge presence	0.29	**0.39***	0.31	0.27	0.22	0.38	0.20	0.19	0.44	−0.42
PUTS	Urge strength	**0.42***	**0.44***	0.29	0.35	0.27	**0.39***	0.25	0.12	0.42	**−0.49***
PUTS	Tic frequency	**0.40***	**0.45***	0.17	**0.37***	**0.40***	**0.44***	0.25	0.23	**0.46***	−0.42
PUTS	Tic control	0.28	0.25	0.16	0.13	0.01	0.01	0.03	−0.11	−0.17	−0.08
CBCL	Anxiety/Depression	**0.45***	**0.48****	0.18	**0.49****	0.24	0.30	0.18	0.21	**0.74****	−0.35
CBCL	Withdrawn	0.40	0.22	−0.01	**0.59****	0.29	0.39	0.37	**0.45***	0.43	−0.23
CBCL	Somatic complaints	0.10	**0.41***	0.23	0.20	0.28	0.31	0.03	0.06	**0.57****	**−0.58****
BRIEF	Emotional control	**0.54****	**0.58****	0.40*	**0.46****	0.15	0.24	0.36	0.36	**0.69****	−0.12

DLPFC = dorsolateral prefrontal cortex, SMA = supplemental motor area, Inf = inferior, YGTSS = Yale Global Tic Severity Scale, PUTS = Premonitory Urge Scale, CBCL = Child Behavior Checklist, BRIEF = Behavioral Ratings of Individual Executive Functions. Bold signifies the * $p < 0.05$ and ** $p < 0.01$.

strong and significant associations between frontal gamma power and parietal alpha power with tic severity and impairment (YGTSS Total and Impairment) emerged. Gamma power in the DLPFC, SMA, and posterior cingulate clusters was also significantly associated with tic frequency and urge strength (PUTS), anxiety/depression (CBCL), and emotional control (BRIEF). These correlations suggest that, in general, higher frontal and parietal spectral power was associated with greater tic severity, stronger premonitory urge and affective dysregulation.

3.4. Connectivity dynamics across ICA-resolved sources during cued voluntary movement

After calculating dipole density for 76 anatomical regions, the CTD and HC groups had 70% overlap of top regions with the highest dipole density, suggesting that similar cortical networks were used across groups to carry out the VM. Given the significant overlap, we focused on the 12 regions shared between the two groups as dominant nodes for the connectivity analysis: bilateral precuneus, bilateral supplemental motor area, bilateral superior frontal cortex, bilateral midcingulate cortex, left (L) cuneus, L precentral, L calcarine, and L superior occipital (see Fig. 4). Despite the overlap, regions of highest dipole density for the HC group were generally in frontal regions (60%), whereas the regions for children with CTD were predominantly posterior (80%).

To determine the group difference in information flow, the subtraction of CTD – HC groups was performed on time-frequency points of the overlapping edges. The results indicated significant information flow increase in CTD group from occipital into the frontal regions after the VM cue (see Supplemental Material, S10 for node analysis). Visual inspection of the full-spectrum results (2–45 Hz) indicated that major modulation of information flows were present in the lower frequency range of 2–13 Hz, which includes delta, theta, and alpha frequency bands, which subsequently became the focus for the effective connectivity analysis.

Analyses of information flow across the graph edges in the 2–13 Hz range indicate that the CTD group exhibited significantly increased information flow compared with HC group. The evolving group dynamics across time can be viewed in two movies from axial and sagittal viewpoints (Supplementary Videos).

A snapshot of the group differences in the 2–13 Hz range from occipital to frontal regions at 420 ms after stimulus onset is depicted in Fig. 5B. The CTD group showed an immediate increase in information flow after the VM cue from occipital to midcingulate and frontal regions, whereas the HC group showed general decrease of information flows relative to the baseline period (Fig. 5C). The same pattern was also found in the edge from the SMA to precuneus, although the magnitude of and group difference in information flow was modest. A closer investigation of the generated movie revealed that there are two peaks in the envelope of information flow time series, one at 140 ms and the other at 420 ms (Fig. 5B, bottom). The first peak is associated with unidirectional information flows from occipital to frontal. However, from 340 ms the information flow between these regions becomes bi-directional, which continues until 440 ms. These observations suggest that the nature of connectivity dysregulation in CTD may be characterized as abnormal increase of 1) initial information flow from occipital to frontal (140 ms) regions, likely representing visual information processing of the cue (Grent-'t-Jong and Woldorff, 2007), and 2) subsequent frontal responses to the occipital region (340–440 ms), critical to motor planning and blink preparation (Deiber et al., 2012), which immediately precedes blink execution at ~600–650 ms.

4. Discussion

Our results provide the first cortical source-resolved, event-related assay of brain oscillatory activity and effective connectivity underlying cued eye blinks in a sample of children (mean age of 9.5 years) with and without CTD. Overall, the EEG results suggest that the CTD group exhibited increased activation of regions related to blink regulation and control (DLPFC, SMA, inferior parietal) as well as those associated with top-down attention processes (DLPFC, posterior cingulate). The brain oscillatory activities in frontal and parietal regions are strongly and significantly associated with clinical characteristics such as tic severity, premonitory urge, emotion regulation and anxiety/depression, suggesting that similar neural mechanisms exert executive control over both visual-motor, attention and emotional responses. Group-level effective connectivity analyses suggest a largely overlapping connectivity network across diagnostic groups, however, children with CTD exhibit network dysregulation, particularly increased information inflow and outflow from posterior to frontal regions, relative to controls.

In terms of brain oscillatory activity, patients with CTD tended to show higher gamma spectral power in SMA, left DLPFC, and posterior cingulate sources relative to controls. High frequency gamma band (30–50 Hz) oscillations reflect a local state of high excitability and synchronization among neuronal assemblies (Hashemiyoon et al., 2017). A recent fMRI study of blink inhibition and control reported increased activity in DLPFC, SMA, precuneus, and cuneus as well as the midcingulate and somatosensory areas (Abi-Jaoude et al., 2018), suggesting children with CTDs required more neural resources than controls for the same level of behavioral performance. A predominant model for CTD dysfunction has been based on insufficient inhibitory motor control due to decreased inhibitory output from the basal ganglia, which may result in frontal cortical hyperactivation as a result of thalamic disinhibition (Albin and Mink, 2006). Thus, cortical dysfunction may be a key mechanism for CTD pathophysiology (Thomalla et al., 2014), consistent with previous reports that the anterior

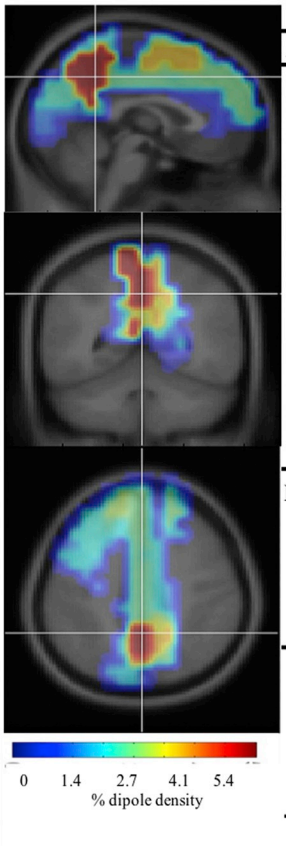

	Combined	HC	CTD
Anatomical ROI labels	%Total Dipole Density		
Precuneus_L	5.41	5.95	5.01
Precuneus_R	3.9	4.57	3.41
Supp_Motor_Area_L	3.79	4.57	2.94
Frontal_Sup_L	3.09	2.32	2.28
Frontal_Sup_R	2.84	3.6	3.65
Cingulum_Mid_L	2.59	3.18	2.16
Cuneus_L	2.36	2.26	2.43
Supp_Motor_Area_R	2.29	3.53	1.01
Cingulum_Mid_R	2.13	2.46	1.89
Precentral_L	2.11	1.93	2.25
Occipital_Sup_L	1.81	1.72	1.87
Calcarine_L	1.24	1.55	1.01
Frontal_Sup_Medial_L	--	2.39	--
Frontal_Mid_L	--	1.46	--
Calcarine_R	--	1.27	--
Lingual_R	--	0.96	--
Cingulum_Ant_L	--	0.69	--
Parietal_Sup_R	--	--	3.41
Postcentral_R	--	--	2.66
Occipital_Sup_R	--	--	1.67
Cuneus_R	--	--	1.63
Cingulum_Ant_R	--	--	0.8
Total variance	33.5	44.8	41.5

Fig. 4. Dipole Density for Tic and Control groups. Pictures on left show Combined dipole density in brain from sagittal, radial and axial views. Percent of dipole density is presented by group and combined. Top regions overlapped by 70%, however the healthy control (HC) group had more frontal regions (60%) and Chronic Tic Disorder (CTD) group had more posterior regions (80%) with the highest dipole density. L = left, R = right, Supp = supplemental, Sup = superior, Ant = anterior.

cingulate cortex, insula and SMA have been implicated in CTDs as they are believed to be important for urge and impulse control (Hallett, 2015). Furthermore, gamma band modulation was recently suggested as a putative biomarker of tic severity, due to a significant correlation with tic severity when deep brain stimulation treatment was applied to the thalamus (Maling et al., 2012). Aberrant glutamate/GABA interneuron signaling, with which gamma band activity has been associated (Hashemiyoon et al., 2017), has also been suggested as a neurochemical basis for tics (Kanaan et al., 2017). Collectively, the activation results suggest that higher frontal gamma power and cortical activation may be a compensatory mechanism needed to override thalamic disinhibition and higher levels of 'neural noise.'

Similarly, greater activation of the posterior cingulate and parietal cortex among individuals with CTDs relative to HC children may represent compensatory mechanisms of visuospatial attention, stimulus evaluation, response selection, motor planning, and internal and external monitoring (Deiber et al., 2012; Baddeley, 2012; Petruo et al., 2018). Suppression of alpha- and beta-band oscillations have been shown to be correlates of active cortical processing, motor planning and inhibitory mechanisms (Foxe and Snyder, 2011; Klimesch et al., 2007) and this was also notably weaker in bilateral inferior parietal regions among children with CTDs relative to the HC group. Both increased alpha coherence and attenuated beta suppression have been reported among adults with CTDs during motor preparation, performance of inhibitory tasks such as the Go/NoGo, and active tic suppression (Niccolai et al., 2016). Posterior alpha has also been linked to cortico-thalamic network activity, making these findings consistent with the prevalent neurobiological theories of Tourette Syndrome that implicate cortico-basal ganglia-thalamo-cortical networks underlying tic generation (Ganos et al., 2013; Jackson et al., 2015). Significant behavioral correlates of aberrant alpha, beta and gamma band spectral power suggest these dynamics are also associated with tic severity, premonitory urge, and emotional dysregulation among children with CTDs.

The connectivity results suggest that overlapping neural networks were used to respond to the VM cue, however, children with CTD had a preponderance of posterior cortical sources (80%) while the majority of active nodes for HC were frontal (60%). These results are highly compatible with recent neuroimaging studies that showed similar small-world organization and hub distributions of white matter tracts but disrupted network integrity, particularly in parieto-occipital cortex, paracentral lobule (mid-cingulate), and precuneus (Wen et al., 2016). These same three regions constituted the dominant nodes and edges in this connectivity analysis, with bilateral precuneus having the highest dipole density for both groups. Thus, decreased structural connectivity and nodal efficiency may underlie greater information flow dysregulation from occipital to frontal/central areas exhibited by children with CTD. These results may support the 'immature brain' hypothesis of CTD (Hashemiyoon et al., 2017; Ghanizadeh and Mosallaei, 2009), which postulates that proper regulation or suppression of information flow and top down control over sensorimotor areas by frontal areas is developmentally delayed among children with CTD. Further support for this hypothesis can be found in a recent meta-analysis of neuroimaging studies of CTD, where only activation in prefrontal and motor preparation regions significantly predicted tic severity (Polyanska et al., 2017). Finally, this hypothesis helps to explain the clinical course of tics and tic severity, which generally lessen into adolescence and adulthood, when frontal lobes are developing for the vast majority of individuals with CTD. Taken together, the connectivity results suggest aberrant interactions and information flow among regions associated with effortful control of blinks such as fronto-occipital pathways as well as attention, sensorimotor integration, and motor planning in children with CTD, the results of which are higher levels of activation and connectivity in order to carry out the cued eye blink.

To our knowledge, this is the first ICA-resolved, event-related assay of brain oscillatory activity and effective connectivity occurring during a cued eye blink paradigm. A limitation of this data is that it may not

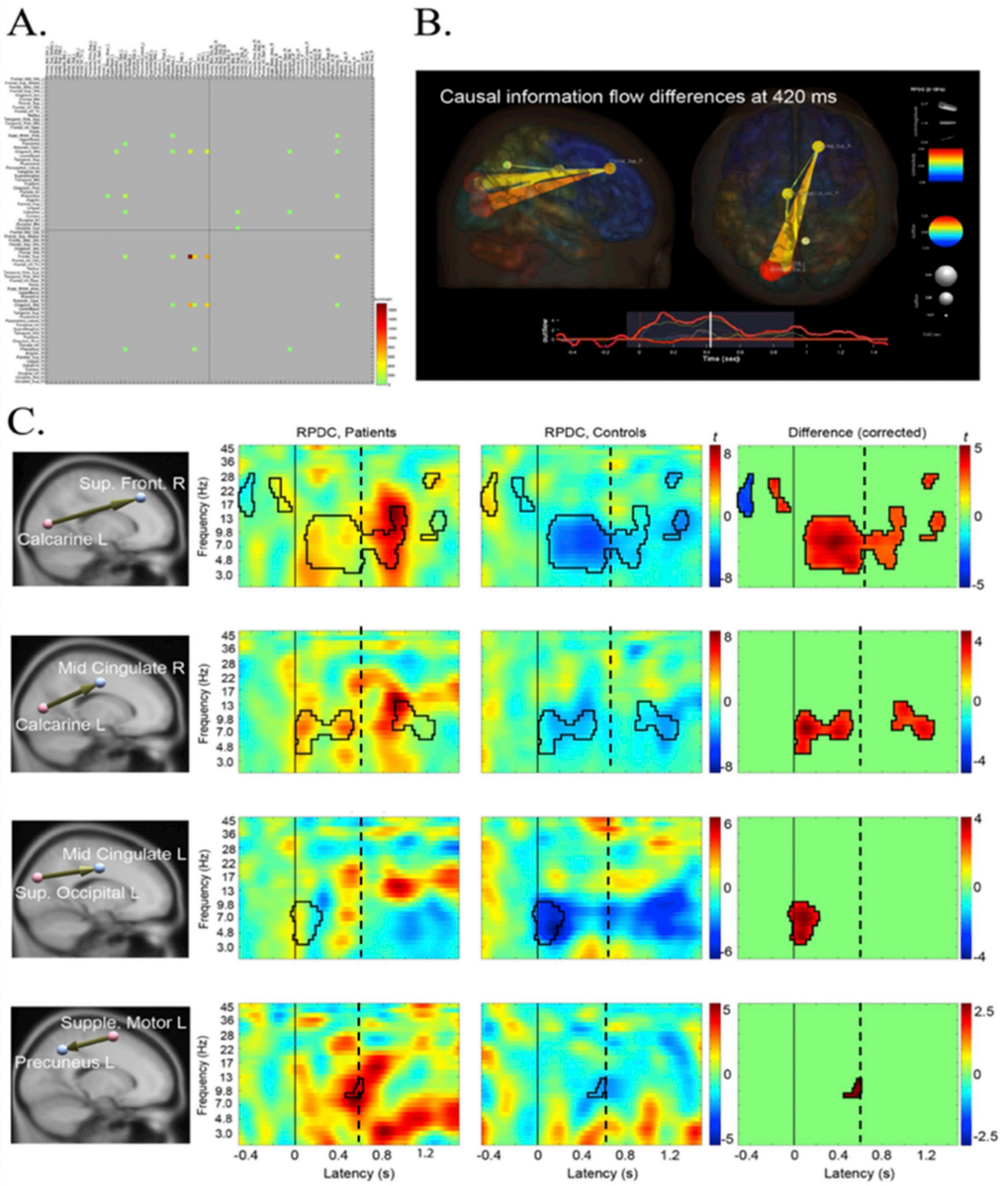

Fig. 5. Connectivity analysis results. A. The connectivity matrix of 76 × 76 anatomical ROIs. Significant edges are color-coded. B. One frame of the information flow movie at 420 ms after the blink cue onset seen from a sagittal and axial views. The bottom panel shows the envelope of the significant edges between 2 and 13 Hz. C. The four most dominant edges showing group differences ($p < .05$). CTD patients failed to suppress information flow from occipital to frontal/central and motor to intraparietal/occipital. Solid black line at Latency = 0 is the blink cue onset. Dotted line indicates mean blink latency. RPDC = renormalized partial directed coherence.

inform the neural mechanisms underlying tic generation, premonitory urge or even voluntary suppression of a tic since mechanisms underlying generation of involuntary and voluntary motor behaviors may be different (Ganos et al., 2018). However, the frontal and parietal activation results were significantly correlated with behavioral ratings of tic severity and premonitory urge, potentially suggesting strong overlap in functionality of these areas within CTD. Second, the cued VM replicates a common tic behavior, eyeblinks, which may increase the relevance of the task but also be confounded by tic activity. ICA performs exceptionally well in extracting eyeblink data, which helps to ensure that the data are minimally affected by EMG, which is always a concern with higher frequency bands such as gamma, and also allows examination of the behavioral task performance. The two groups did not differ significantly in blink number, latency, or ERP amplitude during the VM session, suggesting that extraneous eye blink tics were not likely to be a confound in the current results. Finally, the underlying neurobiology of CTDs is widely noted to involve aberrant subcortical activity within the cortico-striato-thalamo-cortical motor network (Ganos et al., 2013), which EEG is not well suited to detect. However, we note that recent imaging studies and a meta-analysis of task-based neuroimaging studies failed to find significant differences in activation and network disruptions involving basal ganglia or thalamic regions (Wen et al., 2017; Wen et al., 2016). While subcortical activity likely plays a role in tic generation, there are clear cortical dysfunctions that contribute meaningfully to the CTD phenotype that are well assessed by EEG.

In conclusion, this study utilized an innovative mobile brain-body imaging approach (i.e., integrated EEG, EMG, HD video) and a novel voluntary movement paradigm to demonstrate that children with CTDs required higher neural activation and connectivity within regions typically associated with effortful control of cued eye blinks relative to controls, despite similar levels of behavioral performance.

Acknowledgements/Disclosures

Funding for the current study was provided by National Institutes of Neurological Disease and Stroke grants 80160 and 97484 (SKL). The Swartz Center for Neural Computation, directed by Scott Makeig, was founded in 2001 by a generous gift from founding donor Dr. Jerome Swartz of The Swartz Foundation (Old Field, New York). We thank Christian Kothe, Sheng-Hsiou (Shawn) Hsu, and Chiyuan Chang for their help in describing mathematical process of ASR, Nima Bigdely-Shamlo and Tim Mullen for building the framework of groupSIFT application. All authors report no financial conflicts of interest with this work.

Appendix A. Supplementary data

Supplementary data to this article can be found online at https://doi.org/10.1016/j.nicl.2019.101956.

References

Abi-Jaoude, E., Segura, B., Cho, S.S., Crawley, A., Sandor, P., Fall 2018. The neural correlates of self-regulatory fatigability during inhibitory control of eye blinking. J. Neuropsychiatr. Clin. Neurosci. 30 (4), 325–333.
Achenbach, T.M., 2000. Manual for the Child Behavior Checklist/4-18 and 1991 Profile. University of Vermont Department of Psychiatry, Burlington, VT.
Albin, R.L., Mink, J.W., 2006. Recent advances in Tourette syndrome research. Trends Neurosci. 29 (3), 175–182 Mar.
Baddeley, A., 2012. Working memory: theories, models, and controversies. Annu. Rev. Psychol. 63, 1–29.
Barnett, L., Seth, A.K., Oct 15 2011. Behaviour of granger causality under filtering: theoretical invariance and practical application. J. Neurosci. Methods 201 (2), 404–419.
Berman, B.D., Horovitz, S.G., Morel, B., Hallett, M., Aug 30 2011. Neural correlates of blink suppression and the buildup of a natural bodily urge. Neuroimage 59, 1441–1450.
Bloch, M.H., Peterson, B.S., Scahill, L., et al., 2006. Adulthood outcome of tic and obsessive-compulsive symptom severity in children with Tourette syndrome. Arch. Pediatr. Adolesc. Med. 160 (1), 65–69 Jan.
Bodis-Wollner, I., Bucher, S.F., Seelos, K.C., Nov 10 1999. Cortical activation patterns during voluntary blinks and voluntary saccades. Neurology 53 (8), 1800–1805.
Chung, J.Y., Yoon, H.W., Song, M.S., Park, H., Mar 13 2006. Event related fMRI studies of voluntary and inhibited eye blinking using a time marker of EOG. Neurosci. Lett. 395 (3), 196–200.
Chung, J.W., Ofori, E., Misra, G., Hess, C.W., Vaillancourt, D.E., Jan 1 2017. Beta-band activity and connectivity in sensorimotor and parietal cortex are important for accurate motor performance. Neuroimage 144, 164–173 Pt A.
Church, J.A., Fair, D.A., Dosenbach, N.U., et al., 2009. Control networks in paediatric Tourette syndrome show immature and anomalous patterns of functional connectivity. Brain 132 (Pt 1), 225–238 Jan.
Como, P.G., 2001. Neuropsychological function in Tourette syndrome. Adv. Neurol. 85, 103–111.
Deckersbach, T., Chou, T., Britton, J.C., et al., Dec 30 2014. Neural correlates of behavior therapy for Tourette's disorder. Psychiatry Res. 224 (3), 269–274.
Deiber, M.P., Sallard, E., Ludwig, C., Ghezzi, C., Barral, J., Ibanez, V., 2012. EEG alpha activity reflects motor preparation rather than the mode of action selection. Front. Integr. Neurosci. 6, 59.
Delorme, A., Makeig, S., Mar 15 2004. EEGLAB: an open source toolbox for analysis of single-trial EEG dynamics including independent component analysis. J. Neurosci. Methods 134 (1), 9–21.
Delorme, A., Mullen, T., Kothe, C., et al., 2011. EEGLAB, SIFT, NFT, BCILAB, and ERICA: new tools for advanced EEG processing. Comput. Intell. Neurosci. 2011, 130714.
Foxe, J.J., Snyder, A.C., 2011. The role of alpha-band brain oscillations as a sensory suppression mechanism during selective attention. Front. Psychol. 2, 154.
Franzkowiak, S., Pollok, B., Biermann-Ruben, K., et al., 2010. Altered pattern of motor cortical activation-inhibition during voluntary movements in Tourette syndrome. Mov. Disord. 25 (12), 1960–1966 Sep 15.
Franzkowiak, S., Pollok, B., Biermann-Ruben, K., et al., 2012. Motor-cortical interaction in Gilles de la Tourette syndrome. PLoS One 7 (1), e27850.
Ganos, C., Roessner, V., Munchau, A., 2013. The functional anatomy of Gilles de la Tourette syndrome. Neurosci. Biobehav. Rev. 37 (6), 1050–1062 Jul.
Ganos, C., Kahl, U., Brandt, V., et al., 2014. The neural correlates of tic inhibition in Gilles de la Tourette syndrome. Neuropsychologia 65, 297–301 Dec.
Ganos, C., Rothwell, J., Haggard, P., 2018. Voluntary inhibitory motor control over involuntary tic movements. Mov. Disord. 33 (6), 937–946.
Ghanizadeh, A., Mosallaei, S., 2009. Psychiatric disorders and behavioral problems in children and adolescents with Tourette syndrome. Brain Dev. 31 (1), 15–19 Jan.
Gioia, G.A., Isquith, P.K., Retzlaff, P.D., Espy, K.A., 2002. Confirmatory factor analysis of the behavior rating inventory of executive function (BRIEF) in a clinical sample. Child Neuropsychol. 8 (4), 249–257 Dec.
Grent-'t-Jong, T., Woldorff, M.G., Jan 2007. Timing and sequence of brain activity in top-down control of visual-spatial attention. PLoS Biol. 5 (1), e12.
Groppe, D.M., Urbach, T.P., Kutas, M., 2011a. Mass univariate analysis of event-related brain potentials/fields I: a critical tutorial review. Psychophysiology 48 (12), 1711–1725 Dec.
Groppe, D.M., Urbach, T.P., Kutas, M., 2011b. Mass univariate analysis of event-related brain potentials/fields II: simulation studies. Psychophysiology 48 (12), 1726–1737 Dec.
Gwin, J.T., Gramann, K., Makeig, S., Ferris, D.P., 2011. Electrocortical activity is coupled to gait cycle phase during treadmill walking. Neuroimage 54 (2), 1289–1296 Jan 15.
Hallett, M., 2015. Tourette syndrome: update. Brain Dev. 37 (7), 651–655 Aug.
Hashemiyoon, R., Kuhn, J., Visser-Vandewalle, V., 2017. Putting the pieces together in Gilles de la Tourette syndrome: exploring the link between clinical observations and the biological basis of dysfunction. Brain Topogr. 30 (1), 3–29 Jan.
Jackson, G.M., Draper, A., Dyke, K., Pepes, S.E., Jackson, S.R., 2015. Inhibition, disinhibition, and the control of action in Tourette syndrome. Trends Cogn. Sci. 19 (11), 655–665 Nov.
Kanaan, A.S., Gerasch, S., Garcia-Garcia, I., et al., 2017. Pathological glutamatergic neurotransmission in Gilles de la Tourette syndrome. Brain 140 (1), 218–234 Jan.
Klimesch, W., Sauseng, P., Hanslmayr, S., 2007. EEG alpha oscillations: the inhibition-timing hypothesis. Brain Res. Rev. 53 (1), 63–88 Jan.
Leckman, J.F., Riddle, M.A., Hardin, M.T., et al., 1989. The Yale Global Tic Severity Scale: initial testing of a clinician-rated scale of tic severity. J. Am. Acad. Child Adolesc. Psychiatry 28 (4), 566–573 Jul.
Leech, R., Sharp, D.J., 2014. The role of the posterior cingulate cortex in cognition and disease. Brain 137 (Pt 1), 12–32 Jan.
Lerner, A., Bagic, A., Hanakawa, T., et al., 2009. Involvement of insula and cingulate cortices in control and suppression of natural urges. Cereb. Cortex 19, 218–223.
Liu, Y., Miao, W., Wang, J., et al., 2013. Structural abnormalities in early Tourette syndrome children: a combined voxel-based morphometry and tract-based spatial statistics study. PLoS One 8 (9), e76105.
Makeig, S., Bell, A.J., Jung, T.P., Sejnowski, T.J., 1996. Independent component analysis of electroencephalographic data. In: Touretzky, D., Mozer, M., Hasselmo, M. (Eds.), Advances in Neural Information Processing Systems, pp. 145–151.
Maling, N., Hashemiyoon, R., Foote, K.D., Okun, M.S., Sanchez, J.C., 2012. Increased thalamic gamma band activity correlates with symptom relief following deep brain stimulation in humans with Tourette's syndrome. PLoS One 7 (9), e44215.
McGuire, J.F., Piacentini, J., Scahill, L., et al., 2015. Bothersome tics in patients with chronic tic disorders: characteristics and individualized treatment response to behavior therapy. Behav. Res. Ther. 70, 56–63 Jul.
Mullen, T.R., Kothe, C.A., Chi, Y.M., et al., 2015. Real-time neuroimaging and cognitive monitoring using wearable dry EEG. IEEE Trans. Biomed. Eng. 62 (11), 2553–2567 Nov.
Niccolai, V., van Dijk, H., Franzkowiak, S., et al., 2016. Increased beta rhythm as an

indicator of inhibitory mechanisms in tourette syndrome. Mov. Disord. 31 (3), 384–392 Mar.
Oostenveld, R., Fries, P., Maris, E., Schoffelen, J., 2011. FieldTrip: open source software for advanced analysis of MEG, EEG, and invasive electrophysiological data. Comput. Intell. Neurosci. 2011 (Article ID 156869):9 pages).
Palmer, J., Kreutz-Delgado, K., Makeig, S., 2006. Super-Gaussian mixture source model for ICA. In: Paper Presented at: Proceedings of the 6th International Symposium on Independent Component Analysis.
Palmer, J., Kreutz-Delgado, K., Rao, B., Makeig, S., 2007. Modeling and estimation of dependent subspaces with non-radially symmetric and skewed densities. In: Paper Presented at: Proceedings of the 7th International Conference on Independent Components Analysis and Signal Separation, (London, UK).
Peterson, B.S., Staib, L., Scahill, L., et al., 2001. Regional brain and ventricular volumes in Tourette syndrome. Arch. Gen. Psychiatry 58 (5), 427–440 May.
Petruo, V., Bodmer, B., Brandt, V.C., et al., Jun 20 2018. Altered perception-action binding modulates inhibitory control in Gilles de la Tourette syndrome. J. Child Psychol. Psychiatry Epub ahead of print.
Piacentini, J.C., Chang, S.W., 2006. Behavioral treatments for tic suppression: habit reversal training. Adv. Neurol. 99, 227–233.
Polyanska, L., Critchley, H.D., Rae, C.L., 2017. Centrality of prefrontal and motor preparation cortices to Tourette syndrome revealed by meta-analysis of task-based neuroimaging studies. Neuroimage Clin. 16, 257–267.
Roessner, V., Overlack, S., Schmidt-Samoa, C., et al., 2011. Increased putamen and callosal motor subregion in treatment-naive boys with Tourette syndrome indicates changes in the bihemispheric motor network. J. Child Psychol. Psychiatry 52 (3), 306–314 Mar.
Roessner, V., Wittfoth, M., August, J.M., Rothenberger, A., Baudewig, J., Dechent, P., 2013. Finger tapping-related activation differences in treatment-naive pediatric Tourette syndrome: a comparison of the preferred and nonpreferred hand. J. Child Psychol. Psychiatry 54 (3), 273–279 Mar.
Scahill, L., Riddle, M.A., McSwiggin-Hardin, M., et al., Jun 1997. Children's Yale-Brown obsessive compulsive scale: reliability and validity. J. Am. Acad. Child Adolesc. Psychiatry 36 (6), 844–852.
Scahill, L., Sukhodolsky, D.G., Williams, S.K., Leckman, J.F., 2005. Public health significance of tic disorders in children and adolescents. Adv. Neurol. 96, 240–248.
Schelter, B., Timmer, J., Eichler, M., 2009. Assessing the strength of directed influences among neural signals using renormalized partial directed coherence. J. Neurosci. Methods 179 (1), 121–130 Apr 30.
Schlander, M., Schwarz, O., Rothenberger, A., Roessner, V., 2011. Tic disorders: administrative prevalence and co-occurrence with attention-deficit/hyperactivity disorder in a German community sample. Eur. Psychiatry 26 (6), 370–374 Sep.
Serrien, D.J., Orth, M., Evans, A.H., Lees, A.J., Brown, P., 2005. Motor inhibition in patients with Gilles de la Tourette syndrome: functional activation patterns as revealed by EEG coherence. Brain 128 (Pt 1), 116–125 Jan.
Silverman, W.K., Albano, A.M., 1996. The Anxiety Disorders Interview Schedule for DSM-IV Child and Parent Versions. Graywinds Publications, San Antonio, TX.
Specht, M.W., Woods, D.W., Piacentini, J., et al., 2011. Clinical characteristics of children and adolescents with a primary tic disorder. J. Dev. Phys. Disabil. 23 (1), 15–31 Feb.
Storch, E.A., Hanks, C.E., Mink, J.W., et al., 2015. Suicidal thoughts and behaviors in children and adolescents with chronic tic disorders. Depress. Anxiety 32 (10), 744–753 Oct.
Thibault, G., O'Connor, K.P., Stip, E., Lavoie, M.E., 2009. Electrophysiological manifestations of stimulus evaluation, response inhibition and motor processing in Tourette syndrome patients. Psychiatry Res. 167 (3), 202–220 May 30.
Thomalla, G., Jonas, M., Baumer, T., et al., 2014. Costs of control: decreased motor cortex engagement during a Go/NoGo task in Tourette's syndrome. Brain 137 (Pt 1), 122–136 Jan.
Tzourio-Mazoyer, N., Landeau, B., Papathanassiou, D., et al., 2002. Automated anatomical labeling of activations in SPM using a macroscopic anatomical parcellation of the MNI MRI single-subject brain. Neuroimage 15 (1), 273–289 Jan.
Walkup, J.T., Albano, A.M., Piacentini, J., et al., 2008. Cognitive behavioral therapy, sertraline, or a combination in childhood anxiety. N. Engl. J. Med. 359 (26), 2753–2766 Dec 25.
Wen, H., Liu, Y., Wang, J., et al., 2016. Combining tract- and atlas-based analysis reveals microstructural abnormalities in early Tourette syndrome children. Hum. Brain Mapp. 37 (5), 1903–1919 May.
Wen, H., Liu, Y., Rekik, I., et al., 2017. Disrupted topological organization of structural networks revealed by probabilistic diffusion tractography in Tourette syndrome children. Hum. Brain Mapp. 38 (8), 3988–4008 Aug.
Weschler, D., 1999. Wechsler Abbreviated Scale of Intelligence: Manual. Psychological Corporation, San Antonio, Tx.
Woods, D.W., Piacentini, J., Himle, M.B., Chang, S., 2005. Premonitory Urge for Tics Scale (PUTS): initial psychometric results and examination of the premonitory urge phenomenon in youths with tic disorders. J. Dev. Behav. Pediatr. 26 (6), 397–403 Dec.
Yordanova, J., Heinrich, H., Kolev, V., Rothenberger, A., 2006. Increased event-related theta activity as a psychophysiological marker of comorbidity in children with tics and attention-deficit/hyperactivity disorders. Neuroimage 32 (2), 940–955 Aug 15.